Study of nonlinear effects and self-heating in silicon microring resonator including SRH model for carrier recombination

Study of nonlinear effects and self-heating in silicon microring resonator including SRH model for carrier recombination

Marco Novarese[a], Sebastian Romero Garcia[b], Don Adams[c], Jock Bovington[c], and Mariangela Gioannini[a]

[a]Dipartimento di Elettronica e Telecomunicazioni, Politecnico di Torino 10129, Torino, Italy
[b]Cisco Optical GmbH, Nuremberg,Germany,
[c]Cisco Systems, San Jose, CA 95134, USA

ABSTRACT

The comprehension of non-linear effects in silicon is fundamental when designing ring resonator in the Silicon-On-Insulator (SOI) platform. The optical field propagating in the ring waveguide suffers strong absorption due to Two-Photon-Absorption (TPA) and Free-Carrier-Absorption (FCA) whose strength is proportional to the input power in the ring. The free carriers generated via TPA can then heat the device through self-heating.
In this scenario, we present a new method for the modelling of non-linear effects in silicon based ring resonators. Our numerical approach aims to solve the non-linear problem, which couple the variation of refractive index and losses due to TPA, FCA and self-heating, with trap-assisted rate equations based on the Shockley-Read-Hall (SRH) theory. We show for the first time, that the SRH formulation is capable of predicting the dependence of free carrier lifetime on the power circulating in the ring. The new model is validated by comparing simulation results with experimental measurements on a racetrack microring resonator at steady state and in time domain. By the fitting of the experimental results, we determine the surface trap density to be $3 \cdot 10^{12} cm^{-2}$ assuming donor like trap energy level around $0.9eV$. Through time domain simulation we are able to reproduce oscillations in the output power at the through port caused by the interplay of non-linear effects with self-heating.

Keywords: Shockley-Read-Hall, Free-Carrier-Absortpion, Two-Photon-Absorption, Self-hating, Racetrack resonator, Ring resonator, Non-linear effects in Silicon.

1. INTRODUCTION

Nowadays, several studies have established how silicon is affected by non linear effects in both C- and O-band when the injected power is high.[1–4] Two-photon-Absorption (TPA) and Free-Carrier-Absorption (FCA) are the main mechanism responsible for the wavelength shift and distortion of the ring spectral response at steady state when CW input power is just a few milliwatts. In TPA, two photons are absorbed generating an electron-hole pair which cause a change in the refractive index (blue shift) called free-carrier dispersion (FCD). Free carriers also contribute to higher absorption (FCA) rising the overall optical loss and reducing the quality factor of the resonator. The generated carriers recombine releasing the energy in form of heat (self-heating) that increases the temperature in the structure. As a consequence the refractive index changes and causes a red shift of the ring resonance. The amount of spectral distortion of the ring response is thus determined by the density of free-carriers accumulated in the conduction and valence band, and also by the temperature increase, which is proportional to the dissipated power via the thermal impedance of the ring.
Similarly, periodic oscillations of the output power have been observed even with CW injection; these periodic oscillations are due to an instability of the ring caused by the interplay between the temperature increase and free carrier generation and recombination.[5,6]
In order to design rings with minimum non-linear response, we need therefore a precise modelling of the ring spectral response both at steady state and in the time domain. Several works[1–3] have already coupled TPA,

Further author information: (Send correspondence to M.N.)
M.N..: E-mail: marco.novarese@polito.it
M.G.: E-mail: mariangela.gioannini@polito.it

FCA, FCD and self-heating effects into a system of equation. However they all rely on empirical values of carrier lifetimes that are retrieved by fitting experimental measurements.[1–3]

The carrier lifetime in the silicon waveguide core and the ring thermal impedance are two relevant parameters ruling the impact of nonlinear effects on the distorsion of the transmission coefficients and ring instability. Small lifetime implies fast recombination of free carriers and reduction of three carrier absorption, while small thermal resistance limits the temperature increase in the core.

A careful estimation of the carrier lifetime is therefore required to predict non-linear loss and free-carrier dispersion in the ring. The aim of this work is to present a model which includes the Shockley-Read-Hall theory in the formulation of non-linear effects and self-heating to find self-consistently the spectral response of a racetrack resonator in the non-linear regime both in steady state and in time domain. The model details are discussed in section 2. In section 3 the model is validated by comparing measurements of optical transmission spectra and measured oscillating regimes. We show that our model reproduce well both measurement sets.

2. MODEL

We consider a SOI racetrack resonator illustrated in Fig. 1. Here L_c is the coupler length and L_d the length of the straight waveguide, whereas r is the curvature radius. The coupler has a coupling factor κ and a transmission coefficient t. η^2 indicates the coupling loss in the bus-ring coupling region, the power loss per round trip in this region is $\eta^2 \cdot P_{bus}$,[7] with P_{bus} the power entering in the coupler. The power conservation in the bus-ring coupling region leads to $(1-\kappa^2)(1-\eta^2)+\kappa^2(1-\eta^2)+\eta^2 = 1$.

With the introduction of coupling losses, the power transmission coefficients at the through and drop port are written as:

$$\begin{aligned} T_{drop} &= \frac{\kappa^4(1-\eta^2)^2 a}{|1-t^2 a e^{j\theta}|^2} \\ T_{thr} &= t^2 \frac{|1-(1-\eta^2)a e^{j\theta}|^2}{|1-t^2 a e^{j\theta}|^2}. \end{aligned} \tag{1}$$

The optical power circulating in the racetrack waveguide is:

$$P_c = P_{bus} \frac{\kappa^2(1-\eta^2)}{|1-t^2 a e^{j\theta}|^2}. \tag{2}$$

θ is the total phase variation per round trip, generally written as:

$$\theta = \theta_0 + \Delta\theta + \frac{n_g}{c}(\omega_{in}-\omega_0)L, \tag{3}$$

where θ_0 is the phase variation per round trip at the reference angular pulsation ω_0 in linear regime in the waveguide with effective refractive index $n_{eff,0}$ and group refractive index n_g, while ω_{in} is the angular pulsation of the input power. $\Delta\theta(Pc, \Delta T)$ is the total phase variation per round trip due to the non-linear effects and self-heating, ΔT is the temperature variation within the whole structure. The loss of the optical field per round trip is $a = e^{-\alpha_{eff} L/2}$, where α_{eff} accounts for both linear and non linear modal losses. We therefore can express the effective waveguide loss as:

$$\alpha_{eff}(P_c) = \alpha_0 + \Delta\alpha(P_c, n_e, p_e). \tag{4}$$

α_0 is the liner loss term taking into account bend losses and scattering loss. The second part of eq. (4) can be written as $\Delta\alpha(P_c, n_e, p_e) = \alpha_{TPA}(P_c) + \alpha_{FC}(n_e, p_e)$. Here $\alpha_{TPA}(P_c)$ is the modal loss caused by two-photon absorption, which depends on the power propagating in the ring, and α_{FC} is the free-carrier absorption caused the free carrier densities generated by TPA, namely the electron density per unit volume, n_e, in conduction band and hole density per unit volume, p_e, in valence band.[1,8,9] In a similar way we can express the total effective refractive index of the silicon core as $n_{eff}(n_e, p_e, \Delta T) = n_{eff,0} + \Delta n_{eff}(n_e, p_e, \Delta T)$ with Δn_{eff} the effective refractive index variation caused by FCD and self-heating.

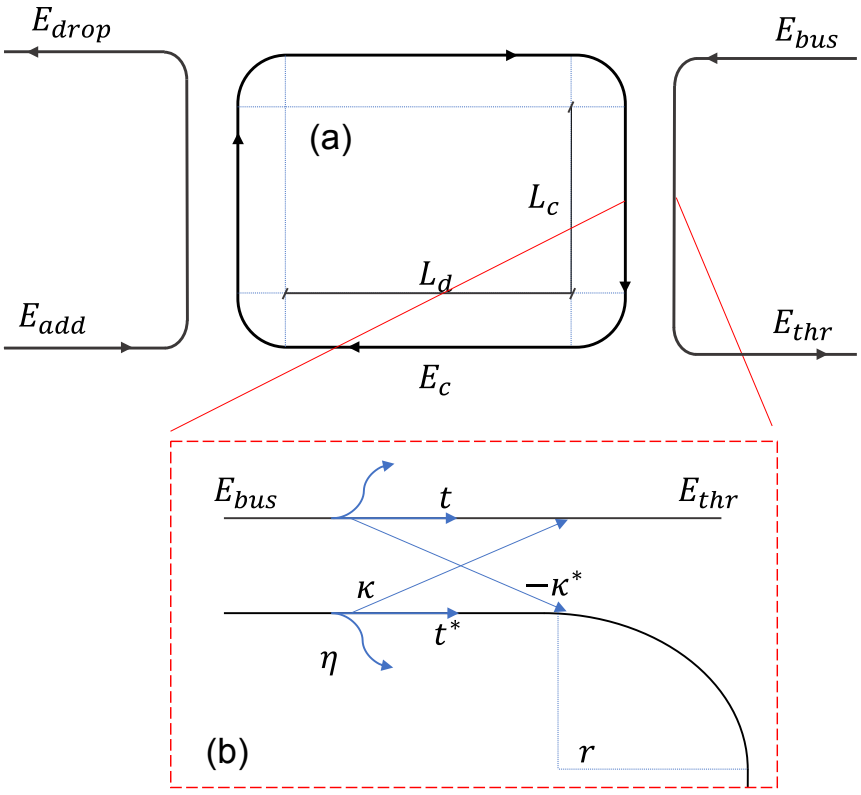

Figure 1: (a) Schematic of the racetrack resonator structure not to scale: here the electric fields at the input bus port (E_{bus}), through port (E_{thr}), add (E_{add}) and drop (E_{drops}) ports are displayed together with the circulating field within the resonator (E_c). The black triangles represent the grating couplers allowing for vertical coupling of light in the ring. In Figure(b) a zoom of the coupler section is displayed.

Generated Free electrons (holes) recombine with free holes (electrons) via Shockley–Read–Hall (SRH) recombination thanks to the presence of trapping states related to defects in the Si bulk material and at the waveguide interface between silica and silicon.
These detrimental processes cause power absorption which is dissipated into heat giving a temperature increase, ΔT, in the silicon core; hence the silicon effective refractive index is modified by the temperature increase caused by self-heating.[1,2,5]
To write the drop and through transmission coefficients as function of the circulating power, FC density and temperature variation, we express the resonant denominator in eq. (1) as function of the ratio $\frac{P_{bus}}{P_c}$:

$$|1 - t^2 a e^{j\theta}|^2 = \frac{P_{bus}}{P_c}\kappa^2(1-\eta^2), \tag{5}$$

and the transmission coefficients of eq. (1) as:

$$\begin{aligned} T_{drop} &= \frac{P_c}{P_{bus}}\kappa^2(1-\eta^2)a \\ T_{thr} &= \frac{P_c}{P_{bus}} \cdot \frac{t^2}{k^2} \cdot \frac{|1-(1-\eta^2)ae^{j\theta}|^2}{(1-\eta^2)}. \end{aligned} \tag{6}$$

To complete the description, we introduce now the Shockley–Read–Hall (SRH) model for carrier recombination which allows us to get an explicit expression for the free carrier density of electrons and holes considering trap recombination.

In,[10] the authors demonstrate that the non-linear carrier dynamics can be well explained in the frame of the rigorous SRH recombination theory.[11] The findings could also justify why in previous works[1–3] it was necessary to assume an empirical carrier lifetime depending on circulating power to explain measured results.

In this work we couple the non-linear ring model with a rigours model of the SRH recombination where the traps act as recombination/trapping center (trap-assisted recombination) upon the capture/trapping of a hole and an electron.

2.1 Model of SRH carrier recombination

The simplest form of expressing free carrier recombination is through a a generic recombination term as $\frac{N}{\tau}$, with N the free carrier density, equal for both holes and electrons, and τ a lifetime for the recombination process. Such formulation implies a constant carrier lifetime which is not true for the silicon waveguide case as experimental measurement on Si straight waveguides[10] showed that FC dynamics is dependent on the optical power in the waveguide and thus the pump power. Following the general theory for SRH recombination,[11] we indicate with N_f the bulk trap density per unit of volume in the silicon waveguide; the latter is associated to surface traps density N_s through the relation $N_f = N_s \cdot \frac{2(W+h)}{W \cdot h}$ where we assume that surface defects are equally distributed over all the contact surface between the silicon core and SiO_2.
We consider donor type traps with non degenerate energy level E_t,[10] which can assume any values between the mid-gap to the bottom of the conduction band.

The free carrier generation rate per unit volume in the waveguide is $G = \frac{\alpha_{TPA} P_c}{2\hbar\omega_{in} A}$, while the rates of variation of excess electron (n_e) and hole (p_e) densities generated by TPA are:[11]

$$\begin{aligned} \frac{\partial n_e}{\partial t} &= G - \frac{1}{\tau_{n0}} \left(\frac{(n_0 + n_1 + n_e)(n_e - p_e)}{N_f} - \frac{n_e n_1}{n_e + n_o} \right) \\ \frac{\partial p_e}{\partial t} &= G - \frac{1}{\tau_{p0}} \left(\frac{(p_0 + p_1 + p_e)(p_e - n_e)}{N_f} - \frac{p_e p_1}{p_e + p_o} \right). \end{aligned} \tag{7}$$

At equilibrium, n_0 and p_0, are the electrons and holes concentration without considering traps; while the quantity of electrons and hole related to the difference between the Fermi level of silicon and trap energy level are expressed as $n_1 = n_0 e^{(E_t - \psi_f)/k_b T}$ and $p_1 = p_0 e^{(\psi_f - E_t)/k_b T}$ respectively.
$\tau_{n0} = (N_f \sigma_n v_n)^{-1}$,$\tau_{p0} = (N_f \sigma_p v_p)^{-1}$ represent the shortest capture time of carriers relative to trapping. $\sigma_{n,p}$ is the capture cross section, and $v_{n,p}$ the thermal velocity of electrons and holes equal to $2.3 \cdot 10^7\, m/s$ and $1.65 \cdot 10^7\, m/s$.[12]

It is important to highlight the difference in capture cross section and thermal velocity of electrons and holes, which cause the capture rate in the traps to unbalance electron and hole densities. As a result the simplifying assumption that $n_e = p_e = N$ fails, even when considering traps exactly at half the bandgap.
The electron capture cross section for donor type trap is a function of the energy of the traps (i.e., $\sigma_n(E_t)$), we extrapolate this function for energies above the mid-gap from measurements reported in.[3] An important quantity to be defined is $\gamma = \tau_{n0}/\tau_{p0}$, which is proportional to the ratio between the two capture cross sections. As reported in the literature,[3,10] it is not possible to measure both the electron and hole capture cross sections when the trap energy level is far from the mid-gap; as a consequence, we suppose $\gamma = 0.05$ as calculated from the ratio of measured cross-sections when E_t is at mid-gap.[3] Once a specific energy trap is chosen, the electron capture cross section is uniquely determined through its energy relation, and the hole cross section by performing $\sigma_p = \gamma \cdot \sigma_n \cdot v_n / v_p$. Lastly, we assume a non-zero residual doping of silicon equal to $N_a = 10^{15}\, cm^{-3}$ corresponding to $\psi_f \approx 0.23\, eV$.

In steady state eq. (7), reduces to two polynomial equations with unknowns n_e and p_e. To ease the calculation, the normalised excess electron and holes densities $y = p_e/p_0$, $x = n_e/p_0$[11] are introduced. In the case of holes,

the associated steady state equation is:

$$\begin{aligned} &y^3 + y^2\left\{(2+b+ab) + N_e b/(1+b) - G_e(1+\gamma^{-1})\right\} + \dots \\ &y\left\{(1+b)(1+ab) + N_e b/(1+b) - G_e/\gamma(1+b)(1+a+2a/\gamma) - N_e G_e(1+2b)/\gamma(1+b)\right\} - \dots \\ &- G_e\left\{(1+b)^2(1+a/\gamma) - N_e(G_e-\gamma)/\gamma^2\right\} = 0. \end{aligned} \tag{8}$$

Where $a = n_1/p_0$, $b = p_1/p_0$, $G_e = G\frac{\tau_{n0}}{p_0}$, $N_e = N_f/p_0$ are all normalised parameters with respect to the hole carrier density at equilibrium.
Eq. (8) can be solved analytically yielding:

$$\begin{aligned} y_k &= \left\{2\sqrt{-\frac{p}{3}}cos\left[\frac{1}{3}\arccos\left(\frac{3q}{2p}\sqrt{-\frac{p}{3}}\right) - 2\pi k/3\right] - \frac{b_y}{3a_y}\right\} \\ p &= \frac{3a_y c_y - b_y^2}{3a_y^2} \\ q &= \frac{2b_y^3 - 9a_y b_y c_y + 27a_y^2}{27a_y^3}, \end{aligned} \tag{9}$$

with $k = 0, 1, 2$. Among the three different solutions, $k = 0$ guarantees the condition $0 < (p_{k,e} - n_{k,e})/N_f < 1$,which represents the fraction of occupied traps, to be satisfied. As a result only this solution is physically acceptable, for this reason the index k is omitted in the remaining discussion being always equal to zero. A similar expression is obtained in the case of electron density.
For any generation rate G_e, we can write an effective electron and hole lifetime defined as:[11]

$$\tau_{n,p} = x, y \cdot \frac{\tau_{n0}}{G_e}. \tag{10}$$

2.2 Steady state model of non-linear loss and self-heating

We are now able to calculate at steady state, thanks to eq. (8) and (**??**) the density of free carriers (electrons and holes) generated for a fixed value of input bus power. The generation of such carriers due TPA causes non-linear loss written as[9] :

$$\alpha_{TPA} = \frac{\beta_{TPA}}{A_{eff}} P_c, \tag{11}$$

where $\beta_{TPA} = 0.8\,cm/GW$ is the TPA absorption coefficient in C-band.[1,8,13,14] The effective area A_{eff} takes into account the portion of area in which the mode interacts with the non linear medium and it is calculated as::[9]

$$A_{eff} = \frac{Z_0^2}{n_{Si}^2} \frac{\left|\int\int_{A_{tot}} \Re e\{E(x,y) \times H(x,y)\} \cdot e_z dxdy\right|^2}{\int\int_A |E(x,y)|^4 dxdy}, \tag{12}$$

where A is the silicon cross section area, A_{tot} the total area of the simulation domain (including both Si and SiO_2 layers) where the electromagnetic field has been computed. $Z_0 = 377\,\Omega$ is the free-space wave impedance. The optical confinement factor (Γ) in the silicon cross section of the waveguide is:[15,16]

$$\Gamma = \frac{n_{Si} c \epsilon_0 \int\int_A |E(x,y)|^2 dxdy}{\int\int_{A_{tot}} \Re e\{E(x,y) \times H(x,y)\} \cdot e_z dxdy}, \tag{13}$$

with e_z the unit vector pointing in the propagation direction z, and $n_{Si} = 3.48$ is the refractive index of Silicon. The modal field distribution $E(x,y)$ and $H(x,y)$ in eq. (12) and (13) are obtained by optical simulation based on the Field-Mode-Matching (FMM) method,[17,18] and cross-checked with a Finite-Element-Method solver.

The modal losses due to free-carrier-absorption are expressed as a function of the excess electron and hole densities obtained by the SRH recombination model, through the empirical expression:[19]

$$\alpha_{FC} = \Gamma\big(8.88 \cdot 10^{-21} n_e^{1.167} + 5.84 \cdot 10^{-20} p_e^{1.109}\big). \tag{14}$$

Free carriers contribute, together with self-heating, to change the effective refractive index as $\Delta n_{eff} = \Delta n_{eff,FCA} + \Delta n_{eff,T}$ with:[19]

$$\Delta n_{eff,FCA} = -\Gamma(5.4 \cdot 10^{-22} n_e^{1.011} + 1.53 \cdot 10^{-18} p_e^{0.838}), \tag{15}$$

obtained experimentally. In both eq. (14) and (15), n_e and p_e are expressed in $[cm^{-3}]$.
For what regards the temperature effect on the refractive index, its derivation is similar to,[1,5] where the variation of temperature inside the ring resonator is computed as:

$$\Delta T = Z_T \cdot P_d, \tag{16}$$

with Z_T being the thermal impedance of the ring, and P_d the power dissipated by the ring. In order to be able to explicitly write such power, we assume that all the optical power lost due to linear and non linear effects is converted into heat,[5] neglecting the irradiated field in the cladding. As a result, for energy balance, P_d is computed as the difference between the input bus power and the power collected at drop and through ports:

$$P_d = (1 - T_{drop} - T_{thr}) \cdot P_{bus}. \tag{17}$$

Lastly the variation of refractive index due to heat generation is:

$$\Delta n_{eff,T} = \Gamma \frac{dn_{Si}}{dT} \Delta T, \tag{18}$$

with $\frac{dn_{Si}}{dT} = 1.86 \cdot 10^{-4}\, K^{-1}$ being the silicon thermo-optic coefficient.[1]
The expressions for the effective loss α_{eff} and phase variation $\Delta\theta$ are a function of P_{bus} and P_c; eq. (2) is a complex non-linear equation with unknown P_c. The latter has been solved numerically for different fixed bus power at any input wavelength λ, and the effective loss and transmission coefficient calculated consequently.
It is important to remind that, the non-linear equation expressed in eq. (2) can have up to three distinct possible solutions,[5] which arise when entering in the so called bi-stable regime. Experimentally the observable cases are those related to a forward and reverse wavelength sweep. A forward sweep is based on increasing the injected wavelength with respect to a previous stable state (i.e., wavelength sweep from blue to red), whereas the reverse one by performing the opposite sweep (from red to blue).[2,5,9]
In the present case we will always consider a forward wavelength sweep performed at different bus power when comparing our model with measured transmission coefficients at steady state.

2.3 Time domain formulation

Non-linear effects are not only detrimental from the steady state point of view; it has been observed that, for high power and pump wavelength close to the resonant frequency, the ring usually enters in an unstable regime characterised by an oscillating output power.[5,6] Such effect originates from the interplay of free carriers and self-heating, which cause the refractive index to oscillate over time. Consequently, the resonant frequency of the ring resonator shifts below and above its cold value periodically with a period of the order of μs.
The strength and period of these oscillations depend on the ring thermal properties (thermal capacitance C_i and impedance Z_i) and on the free carrier density.
We thus extend the previously introduced model to the temporal domain similarly to what done in.[5,6] In particular equations (11), (14),(15), and (18) still holds, however the circulating power $P_c(t)$, $n_e(t)$, $p_e(t)$, and the temperature variation $\Delta T(t)$ are now time dependent.
The differential equation of the circulating field E_c in the racetrack can be obtained through the inverse Fourier transform of eq. (2) by performing the Taylor expansion of $e^{j\cdot\theta}$ around θ_0; the reference pulsation ω_0 corresponds to the cold ring resonance such that $e^{j\cdot\theta_0} \approx 1$. Expressing the circulating field in the ring as $E_{ring}(t) = E_c(t) \cdot e^{(-j\cdot\omega_0 t)}$, we get the equation of E_c:

$$\frac{\partial E_c}{\partial t} = -\left(\frac{\kappa \cdot \sqrt{1-\eta^2}}{t^2 a} E_{in} + E_c(t)(\frac{1}{t^2 a} - 1) + j \cdot \frac{L}{c} \Delta\omega_r \cdot E_c(t)\right) / \tau_g, \tag{19}$$

with $P_{in} = |E_{in}|^2$,$P_c = |E_c|^2$, $\Delta\omega_r = \omega_0 \cdot \Delta n_{eff}$, and $\tau_g = L \cdot n_g / c$.
In eq. (19), the round trip loss a and $\Delta\omega_r$ are time dependent when the ring is not stable, because the carrier density in eq. (7) and temperature may oscillate with time.

The temperature dynamic is written as[5,6]

$$\frac{\partial \Delta T_i(t)}{\partial t} = -\frac{\Delta T_i(t)}{Z_i \cdot C_i} + \frac{P_d(t)}{C_i}. \tag{20}$$

Which at steady state, $\frac{\partial \Delta T_i(t)}{\partial t} = 0$, reduces to eq. (17). ΔT_i is the temperature variation at each node of the equivalent electrical circuit called Foster model[20] shown in Figure 2; the total temperature increase in the silicon core is then $\Delta T(t) = \sum_i^n \Delta T_i(t)$.

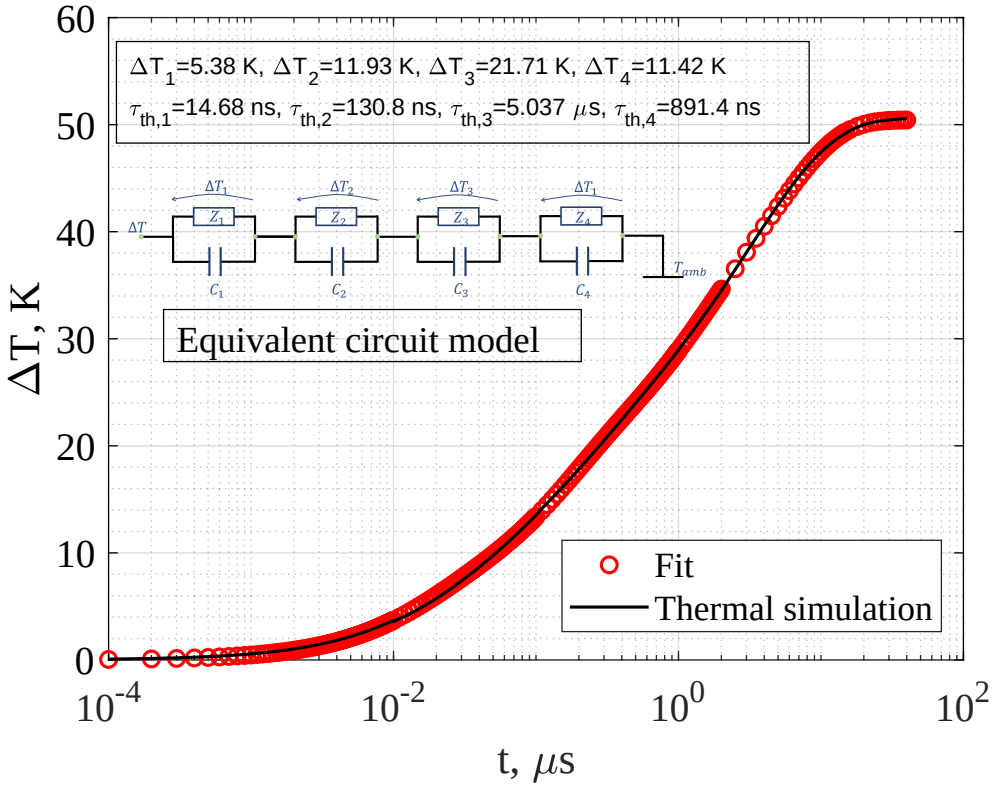

Figure 2: Temperature variation obtained from thermal transient simulation of the complete racetrack resonator, note that in thermal simulation the dissipated power is set to $10mW$, hence the thermal impedance is generally calculated from the steady state temperature variation as as $Z = \Delta T / 10mW$.[5] In the inset the schematic of the equivalent circuit model is displayed with the values of the four thermal impedances and time constants used for the fitting of the thermal transient.

In the Foster model, the total temperature variation in time in the device is expressed as:

$$\Delta T(t) = \sum_i^n \Delta T_i \cdot \left(1 - e^{\frac{t}{Z_{T,i} C_i}}\right), \tag{21}$$

where ΔT_i is the temperature variation at each node i, which is related to the thermal impedance as $Z_i = \Delta T_i/10mW$. The equivalent circuit is composed of a series of n nodes attributed to the complex heat flow between the stack of different Si and SiO_2 layers in the device structure; each node is the result of the parallel between Z_i and C_i,[20] whose product represents the thermal time constant, i.e., $\tau_{th,i} = Z_{T,i}C_i$.[2,5,6] The values for Z_i and C_i can be calculated by fitting transient thermal simulation obtained by means of a commercial thermal solver. We report in Figure 2 the temperature variation in the ring when at $t = 0$ we start to dissipate $10mW$ of power in the silicon waveguide core. It is clear that 4 nodes provide already a good fitting; in addition the shortest thermal relaxation lifetime is calculated to be as small as $14ns$, which we assume to be related to the heat propagation in the silicon core and often neglected in the literature,[5] where instant heating propagation is considered.

The system of ordinary differential equations formed by eq. (7), (19), and (20), for i which goes from 1 to 4 represent the total 7 differential equations to be solved for any input power.
In the following sections, experimental and theoretical results addressing both the steady state and time domain oscillations are presented .

3. RESULTS

To validate our model, in this section we analyse the transmission spectrum and oscillating characteristics of a racetrack resonator. The ring details such as the waveguide cross section, length and coupling coefficients κ^2 are summarized in Table 1.

Parameter	Racetrack resonator ($\lambda_0 = 1540.315nm$)	Unit	Source
L	80	μm	-
W	450	nm	-
h	215	nm	-
Γ	1	-	Electromagnetic mode solver.
A_{eff}	0.075	μm^2	eq. (12)
$n_{eff,0}$	2.33	-	Electromagnetic mode solver
n_g	4.26	-	Electromagnetic mode solver
κ^2	0.066	-	Fitting of $T_{thr}(\lambda)$ in linear regime
α_0	1.995	dB/cm	Fitting of $T_{thr}(\lambda)$ in linear regime
η^2	0.013	-	Fitting of $T_{thr}(\lambda)$ in linear regime
Q	8492	-	Fitting of $T_{thr}(\lambda)$ in linear regime
Z_T	5044	K/W	Thermal simulation

Table 1: Parameters used in the model retrieved from low power fitting, electromagnetic mode solver and thermal simulation.

3.1 Steady state analysis

We measured the output power at the through port of the racetrack resonator by injecting light of an Agilent 81980A tunable laser amplified with an erbium doped fiber amplifier (EDFA). In this way powers we were able to reach powers entering in the ring as high as $7dBm$.
The transmission coefficient at the through port is then measured as the ratio between the measured output power and the power in the bus. Such spectrum is obtained by a forward wavelength sweep around one selected resonant wavelength of the ring λ_0. The sweeping rate is $4pm/s$.
Fig.3 (a) and 3 (b) show the shift of the resonant frequency, $\Delta\lambda = \lambda_{res} - \lambda_0$, and transmission coefficient at resonance extracted from the measured transmission spectra reported in Fig. 3 (c), versus the input bus power in mW. Here the red circles are associated to several measurements made on the ring in similar environmental conditions.

We fitted the spectrum calculated at $P_{bus} = 3dBm$, shown in Figure 3 (c), in order to extract the coupling parameters $\kappa^2, \eta^2, \alpha_0$ summarised in table 1 assuming the ring to be in linear regime. The value for linear losses α_0 has been varied between $1.6dB/cm$ and $2dB/cm$ which represent the typical range of linear losses provided by the foundry for the fabrication.

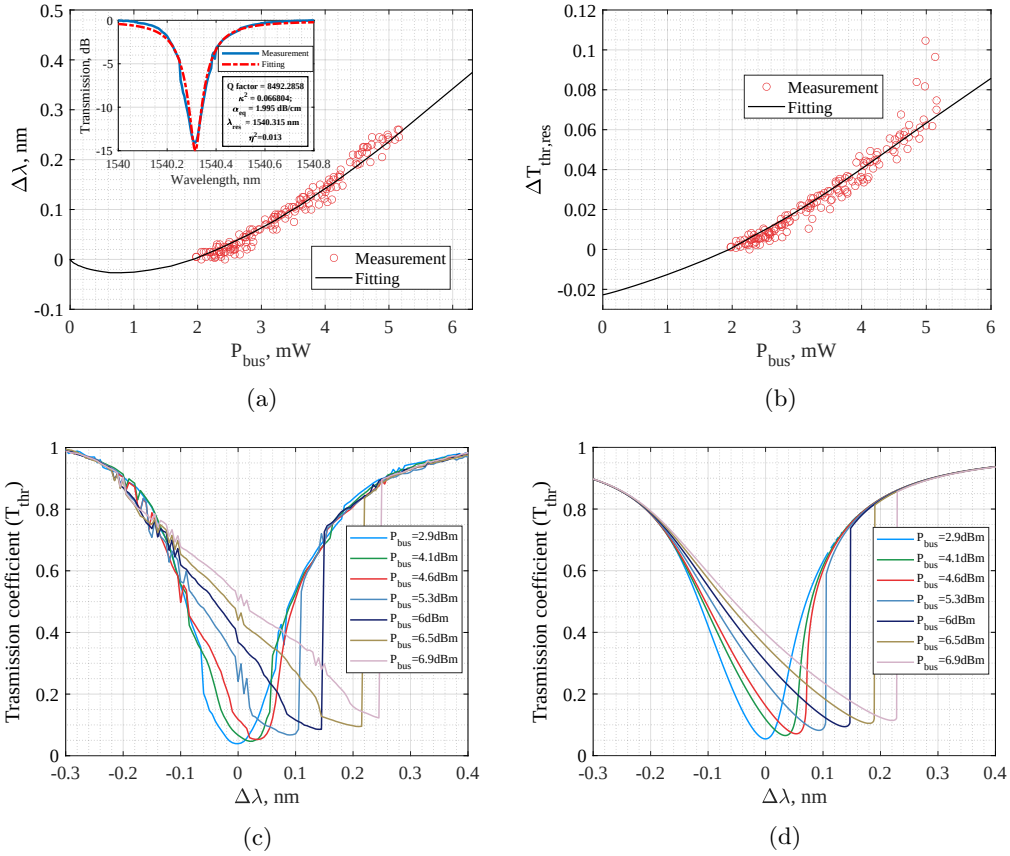

Figure 3: Resonant wavelength shift $\Delta\lambda$ (a) and transmission coefficient variation at resonance (b) as a function of the input bus power. In the inset, low power fitting of the experimental transmission coefficient. The red circles represent values of different measurements in approximately the same coupling conditions. Example of transmission coefficients at different input bus power measured (c) and simulated (d) by sweeping the input wavelength from the blue to red side of the resonant wavelength.

We fit with the theoretical model reported in section 2.1 and 2.2 the measurements in Fig. 3 (a)-(b). The fitting procedure is based on the search for the values of N_f and E_t that minimize the relative error defined as the difference between the measured and simulated variation of resonant wavelength and transmission coefficient. The displayed simulation results in black line in Fig. 3 (a)-(b) were obtained with $N_f = 4.56 \cdot 10^{17}\, cm^{-3}$ and energy gap around $E_t = 0.937\, eV$. The choice of these parameters is unique when fitting both the wavelength and transmission shift, the electron capture cross section is therefore $\sigma_n = 1.64 \cdot 10^{-17} cm^2$. The calculated surface trap density is then $N_s = 3.32 \cdot 10^{12}\, cm^{-2}$, which is close to what is found typically in the literature in the case of a straight waveguide with trap in the mid-gap, i.e. $10^{11} - 10^{12} cm^{-2}$.[10]
With this set of parameters, the simulated transmission spectra is shown in Fig.3 (d) in comparison with a set of measured spectra displayed in Fig. 3 (c) for different bus input powers. With increasing P_{bus}, the circulating power cause higher propagation loss and variation of silicon refractive index within the silicon core. These first result in a slight blue shift of the resonant wavelength, see Figure 3 (a), due to FCD being dominant over the temperature rise effect on the refractive index; then a significant red shift caused by self-heating appears. Figures 3 (a), (b) and (d) show that the model can reproduce well the measured results at steady state thanks to the SRH theory.

In figure 4 (a) we report the the effective lifetimes of carriers in the core of the ring; we observe that, as consequence of the asymmetric capture cross sections an thermal velocities, the two lifetimes are different and

dependent on the circulating power. The trend of the computed non linear carrier lifetime at steady state is in line with other studies[1–3] where the carrier lifetime was assumed to be power dependent to explain experimental findings.

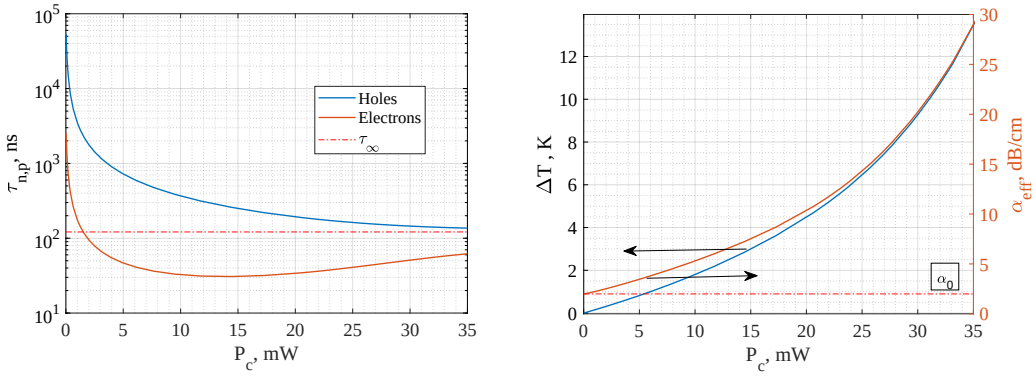

(a) (b)

Figure 4: Electron and holes effective lifetime (a), temperature variation and total losses in the ring (b) as a function of the circulating power. The dashed line in (b) indicates the level of linear loss. The black vertical line represents the circulating power caluclated with $P_{bus} = 3dBm$.

The steady state carrier density is the balance between the increase of the TPA generation rate, which is proportional to the increase of P_{bus}, and the capture rate in the traps. As a consequence, the carrier density does not follow the generation rate, as the rate for a trap to recombine a captured electron / hole pair increases due to the greater number of carriers available. The overall result will be a decreasing carrier lifetime, which is what is seen in the case of the hole carrier density in Fig. 4 (a). In particular, the energy level of the trap, the capture cross section, the doping and the temperature determine how these effective lifetimes depend on P_c. It is interesting to note that the trap energy gap closer to the CB than the VB is the origin for the much faster capture of electrons with respect to holes.
As a result, the created electrons are more easily trapped than holes, in the case of low power they recombine very slowly due to the small availability of holes capable of reaching the trap state, thus they may return to the conduction band leaving the traps behind empty again.[21] This process, further enhanced by having a n-type trap in a p-type silicon waveguide, causes a reduction of the carrier recombination rate, which translates in a higher lifetime for both holes and electrons. For very large power, both $\tau_{n,p}$, eq. (10), will tend to a constant value defined as $\tau_\infty = \tau_{n0}(1 + \gamma^{-1})$ which is equal for both electrons and holes. In this limit the generation is so high that the number of generated free-carriers exceeds the total quantity of traps which become all filled (saturated traps); in our case $\tau_{p,e,\infty} = 121ns$.
Lastly, Figure 4 (b) reports the calculated temperature increase and effective losses(see eq. (4)) at resonance versus the circulating power in the silicon core. Here the dashed red line represents the linear losses in the ring.

3.2 Dynamic response

Figure 5 (a) shows the normalised electrical signal recorded at optical receiver (with 1.1 GHz bandwidth) collecting the output power at the thorough port of the ring. The bus input power is calculated to be around $11dBm$ with $\lambda_{in} \approx \lambda_0$. To get such an high value of bus power, another EDFA, with higher amplification, has been utilised.

As it is possible to see, the recorded signal is not constant when we inject CW input power. Because the input power is high enough and the pump wavelength rather close to the cold resonance frequency, we measure stable oscillations. The measured trace in Fig. 5 (a) in line with experimental results from other studies.[5,6]
Figure 5 (b) reports the results obtained by applying the model of section 2.3 and assuming for the ring the parameters calculated from the fitting of the steady state measurements. In both figures the transmissions have

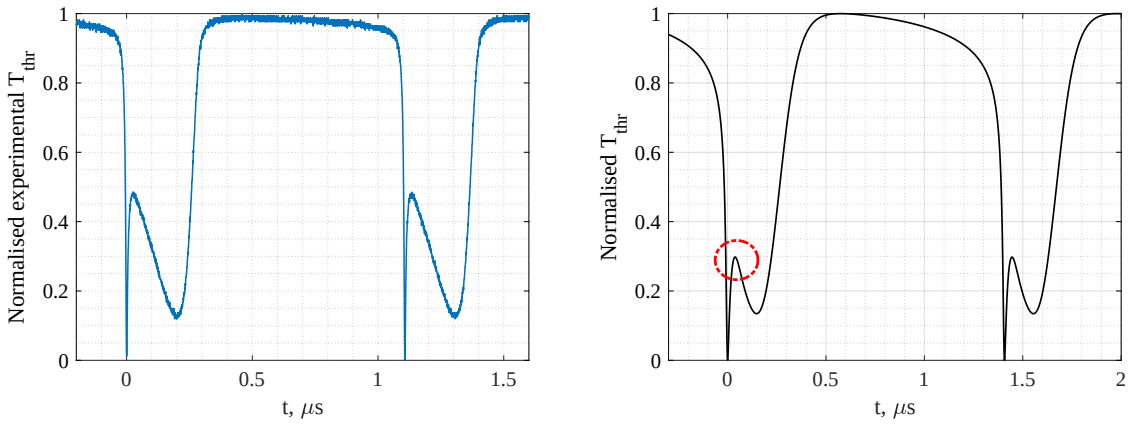

(a) (b)

Figure 5: (a) Normalised measured output signal versus time by the optical receiver at the through port for an input bus power equal to approximately $11dBm$. (b) Normalised model response at the through port injecting the same bus power of $11dBm$.

been normalised as done in [6]. The comparison of Figs. 5 (a) and (b) shows that the model can reproduce quite well the periodic oscillations of the output power with a measured period of $1.1\mu s$ in the experiment and $1.4\mu s$ in simulations.

Some discrepancy is observed in the temporal region highlighted by the red circle in the simulated time traces. This mismatch can be attributed to a possible experimental misalignment of the pump wavelength with the cold resonant frequency. In addition the thermal time constant indicates the speed at which free carriers cause the build up of the self-heating inside the ring: a smaller $\tau_{th,i}$ would produce a faster thermal dissipation affecting the overall signal period and relative position of the different peaks.

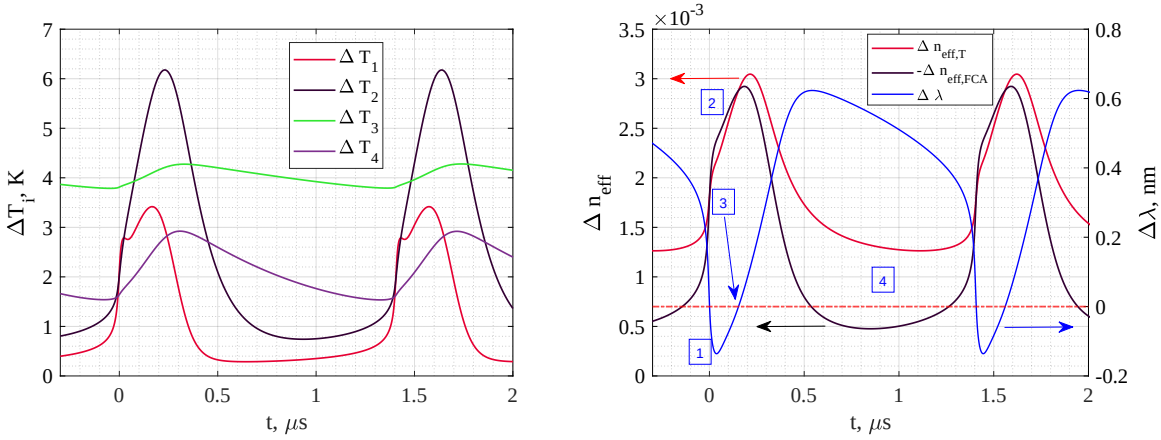

(a) (b)

Figure 6: (a)Temperature variation of the four nodes that form the equivalent thermal circuit. (b) FCA and temperature contributions to the effective refractive index in the silicon core (left), on the right the variation of the resonant wavelength $\Delta\lambda$ within the racetrack resonator over time is shown. The red dashed line in (b) denotes the case when the resonance of the ring is equal to its cold value, i.e., $\lambda_{res} = \lambda_0$.

To explain the measured trace in Fig. 5 we compare in Fig.6 (a) the temperature contributions of the four thermal nodes being part of the equivalent circuit illustrated in Fig. 2. The nodes that exhibit longer thermal

time constants, i.e., ΔT_2 and ΔT_3, need a longer amount of time with respect to the other two to dissipate the heat caused by self-heating. The overall effect of these 4 temperatures on the refractive index, $\Delta n_{eff,T}$, is shown in Fig. 6 (b) along with the contribution of free-carriers to the effective refractive index change. To compare the strength of these two effects, $\Delta n_{eff,FCA}$ is reported with reversed sign.
Analyzing the total variation of the resonance wavelength we identify four regions marked with numbers (1 to 4) in Fig. 6 (b). In the time range marked with (1) the pump wavelength and cold resonant frequency are almost aligned causing a large increase in circulating power, this leads to FC generation responsible for a blue shift of the resonant frequency (FCD) which cause the pump and cold frequency to misalign resulting in a rapid decrease of circulating power. In the meantime, the self-heating, originated by FC absorption, starts red shifting the resonance to its cold value (2). During this process, both FCD and self-heating increase in strength due to carriers generated by the rise in circulating power as the ring resonance is approaching again the cold resonance. However, once the ring resonance is again at the cold resonance (3), the maximum achievable circulating power is lower than in the initial case (1), because the Q factor is greatly degraded by the presence of many free carriers. The absorbed carriers translate into further heat dissipation making the resonance keep on shifting towards the red. Thus P_c decreases and therefore also the carriers generated. In time interval (4) the ring slowly cools down to the initial state once the slowest thermal dissipation process concludes; here P_c increases again and the whole process restarts.
The complete behaviour of n_e, p_e, P_c and thermal dissipation explained above are all in agreement with the literature,[5,6] indicating that the model can be used to explain the experimental results even in time domain.

4. CONCLUSION

We have presented a new approach for the description of TPA, FCA and self-heating in silicon ring resonator by including the Shockley–Read–Hall theory. In addition, we have demonstrated that free carrier lifetime is dependent on the power circulating in the ring through trap-assisted recombination. Thanks to this assumption, we were able to fit the distortion of the ring transmission spectra with increasing input power at steady state and also reproduce periodic oscillation in the ring resonator transmission at the through port with CW input power. For power in the bus waveguide in the range $2 - 6dBm$, the hole lifetime turned out to be approximately one order of magnitude larger than electron lifetimes. Thereby, the hole density is significantly higher than the electron density, suggesting that holes are the main source of free-carrier absorption and dispersion in the analysed racetrack resonator. In summary, our results proved to be in accord with previously published papers, but in this work they have been obtained without any empirical expressions for the carrier lifetime. From this analysis we deduce that surface trap densities around $10^{12}cm^{-2}$ play a remarkable role in defining the trap-recombination process of holes and electrons in sub-micron waveguides. We therefore believe that this model may provide new insight into the development of a tool for the design of narrow band silicon photonic mirrors for hybrid III-V high power tunable lasers.

Founding

This work is funded by a CISCO Sponsored Research Agreement.

REFERENCES

[1] Barclay, P. E., Srinivasan, K., and Painter, O., "Nonlinear response of silicon photonic crystal microresonators excited via an integrated waveguide and fiber taper," *Opt. Express* **13**, 801–820 (Feb 2005).

[2] Priem, G., Dumon, P., Bogaerts, W., Thourhout, D. V., Morthier, G., and Baets, R., "Optical bistability and pulsating behaviour in silicon-on-insulator ring resonator structures.," *Opt. Express* **13**, 9623–9628 (Nov 2005).

[3] Aberle, A. G., Glunz, S., and Warta, W., "Impact of illumination level and oxide parameters on shockley–read–hall recombination at the si-sio2 interface," *Journal of Applied Physics* **71**(9), 4422–4431 (1992).

[4] Xu, Q. and Lipson, M., "Carrier-induced optical bistability in silicon ring resonators," *Opt. Lett.* **31**, 341–343 (Feb 2006).

[5] Soltani, M., *Novel Integrated Silicon Nanophotonic Structures using Ultra-high Q Resonators*, PhD thesis, Georgia Institute of Technology (2009).

[6] Johnson, T., *Silicon Microdisk Resonators for Nonlinear Optics and Dynamics*, PhD thesis, California Institute of Technology (2009).

[7] Tseng, C.-W., Tsai, C.-W., Lin, K.-C., Lee, M.-C., and Chen, Y.-J., "Study of coupling loss on strongly-coupled, ultra compact microring resonators," *Opt. Express* **21**, 7250–7257 (Mar 2013).

[8] Liang, T. K. and Tsang, H. K., "Role of free carriers from two-photon absorption in raman amplification in silicon-on-insulator waveguides," *Applied Physics Letters* **84**(15), 2745–2747 (2004).

[9] Koos, C., Jacome, L., Poulton, C., Leuthold, J., and Freude, W., "Nonlinear silicon-on-insulator waveguides for all-optical signal processing," *Opt. Express* **15**, 5976–5990 (May 2007).

[10] Aldaya, I., Gil-Molina, A., Pita, J. L., Gabrielli, L. H., Fragnito, H. L., and Dainese, P., "Nonlinear carrier dynamics in silicon nano-waveguides," *Optica* **4**, 1219–1227 (Oct 2017).

[11] Blakemore, J., [*Semiconductor Statistics*], Dover Books on Physics Series, Dover (2002).

[12] ioffe.ru, "Electrical properties of silicon(si)," *http://www.ioffe.ru/SVA/NSM/Semicond/Si/* .

[13] Bristow, A. D., Rotenberg, N., and van Driel, H. M., "Two-photon absorption and kerr coefficients of silicon for 850–2200nm," *Applied Physics Letters* **90**(19), 191104 (2007).

[14] Dinu, M., Quochi, F., and Garcia, H., "Third-order nonlinearities in silicon at telecom wavelengths," *Applied Physics Letters* **82**, 2954 – 2956 (06 2003).

[15] Robinson, J. T., Preston, K., Painter, O., and Lipson, M., "First-principle derivation of gain in high-index-contrast waveguides," *Opt. Express* **16**, 16659–16669 (Oct 2008).

[16] Visser, T., Blok, H., Demeulenaere, B., and Lenstra, D., "Confinement factors and gain in optical amplifiers," *IEEE Journal of Quantum Electronics* **33**(10), 1763–1766 (1997).

[17] Sudbo, A. S., "Film mode matching: a versatile numerical method for vector mode field calculations in dielectric waveguides," *Pure and Applied Optics: Journal of the European Optical Society Part A* **2**, 211–233 (may 1993).

[18] de zutter, D., Lagasse, P., Buus, J., Young, T., and Dillon, B., "Comparison of different modelling techniques for longitudinally invariant integrated optical waveguides," *IEE Proceedings J: Optoelectronics* , 273–280 (10 1989).

[19] Nedeljkovic, M., Soref, R., and Mashanovich, G. Z., "Free-carrier electrorefraction and electroabsorption modulation predictions for silicon over the 1–14-μm infrared wavelength range," *IEEE Photonics Journal* **3**(6), 1171–1180 (2011).

[20] Schütze, "Thermal equivalent circuit models. application note. v1.0.," *Infineon Technologies AG* (2008).

[21] Ding, W., Dmitri, D., and et al., J. S., "Carrier lifetime measurements in long-wave infrared inas/gasb superlattices under low excitation conditions.," *Journal of Electronic Materials* **41**, 3027–3030 (2012).